

Convex Relaxations of Chance Constrained AC Optimal Power Flow

Andreas Venzke, *Student Member, IEEE*, Lejla Halilbasic, *Student Member, IEEE*, Uros Markovic, *Student Member, IEEE*, Gabriela Hug, *Senior Member, IEEE*, and Spyros Chatzivasileiadis, *Member, IEEE*

Abstract—High penetration of renewable energy sources and the increasing share of stochastic loads require the explicit representation of uncertainty in tools such as the optimal power flow (OPF). Current approaches follow either a linearized approach or an iterative approximation of non-linearities. This paper proposes a semidefinite relaxation of a chance-constrained AC-OPF which is able to provide guarantees regarding global optimality. Using a piecewise affine policy, we can ensure tractability, accurately model large power deviations, and determine suitable corrective control policies for active power, reactive power, and voltage. We state a tractable formulation for two types of uncertainty sets. Using a scenario-based approach and making no prior assumptions about the probability distribution of the forecast errors, we obtain a robust formulation for a rectangular uncertainty set. Alternatively, assuming a Gaussian distribution of the forecast errors, we propose an analytical reformulation of the chance constraints suitable for semidefinite programming. We demonstrate the performance of our approach on the IEEE 9, 24 and 118 bus system using realistic day-ahead forecast data and obtain tight near-global optimality guarantees.

Index Terms—Convex optimization, AC optimal power flow, semidefinite programming, uncertainty, chance constraints.

I. INTRODUCTION

POWER system operators have to deal with higher degrees of uncertainty in operation and planning. If uncertainty is not explicitly considered, increasing shares of unpredictable renewable generation and stochastic loads, such as electric vehicles, can lead to higher costs and jeopardize system security. The scope of this work is to introduce a convex AC-OPF formulation which is able to model with high accuracy the effect of forecast errors on the power flow, can define a-priori suitable corrective control policies for active power, reactive power, and voltage, and can provide near-global optimality guarantees.

A. Literature review

Chance constraints are included in the OPF formulation to account for uncertainty in power injections, defining a maximum allowable probability of constraint violation. It is generally agreed that the non-linear nature of the AC-OPF along with the probabilistic constraints render the problem for most instances intractable [1]. To ensure tractability of

these constraints, either a data-driven or scenario-based approach is applied or the assumption of specific uncertainty distributions is required for an analytical reformulation of the chance constraints. To deal with the higher complexity of chance constrained OPF, existing approaches either assume a DC-OPF [2]–[6], a linearized AC-OPF [7]–[10] or solve iteratively linearized instances of the non-linear AC-OPF [11], [12]. Chance-constrained DC-OPF results to a faster and more scalable algorithm, but it is an approximation that neglects losses, reactive power, and voltage constraints and can exhibit substantial approximation errors [13].

Refs. [2] and [3] formulate a chance constrained DC-OPF assuming a Gaussian distribution of the forecast errors. The work in [2] relies on a cutting-plane algorithm to solve the resulting optimization problem, whereas the work in [3] states a direct analytical reformulation of the same chance constraints. This framework is further extended by the work in [4] which assumes uncertainty sets for both the mean and the variance of the underlying Gaussian distributions to obtain a more distributionally robust formulation. The work in [5] formulates a robust multi-period chance-constrained DC-OPF assuming interval bounds on uncertain wind infeeds. These works [2]–[5] include corrective control of the generation units to restore the active power system balance as a function of the forecast errors. The work in [6] extends this corrective control framework to HVDC active power set-points and phase shifting transformers in an N-1 security context.

Alternatively, the works in [7]–[10] use a linearization of the AC power flow equations based on [14] to achieve a tractable formulation of the chance constraints. As the operating point is not known a-priori, the linearization is performed around a flat start or no-load voltage, and not the actual operating point. These works [7]–[10] focus on low-voltage distribution systems with high share of photovoltaic (PV) production and minimize PV curtailment subject to chance constraints on voltage magnitudes. Scenario-based methods are applied to achieve a tractable formulation. In this framework, line flow limits and corrective control from conventional generation are not considered. The utilized linearization is designed for radial distribution grids and assumes no voltage control capability of generation units.

In Ref. [11], an iterative back-mapping and linearization of the full AC power flow equations is used to solve the chance constrained AC-OPF. The recent work in [12] uses an iterative procedure to calculate the full Jacobian, which is the exact AC power flow linearization around the operating point. Assuming a Gaussian distribution of the forecast errors, an analytical

A. Venzke, L. Halilbasic and S. Chatzivasileiadis are with the Center for Electric Power and Energy, Technical University of Denmark, 2800 Kgs. Lyngby, Denmark.

U. Markovic and G. Hug are with the Power Systems Laboratory, ETH Zurich, 8092 Zurich, Switzerland.

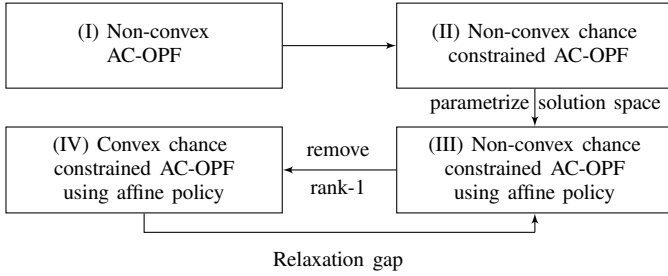


Fig. 1. We restrict the solution space of the non-linear chance constrained AC-OPF to the parametrization by the affine policy. This problem is relaxed by dropping the non-convex rank constraint. With relaxation gap we refer to the gap between problems (IV) and (III).

reformulation of the chance constraints on voltage magnitude and current line flow is proposed. Although this approach can be shown to scale well, it is not convex and does not guarantee convergence.

In this work, we formulate a convex relaxation of a chance-constrained AC-OPF which allows us to provide guarantees for the optimality of the solution, or otherwise determine the distance to the global optimum of the original non-linear problem. Besides that, we include chance constraints for all relevant state variables, namely active and reactive power, voltage magnitudes and active and apparent branch flows. Two tractable formulations of the chance constraints are proposed. First, based on realistic forecast data and making no prior assumptions about the probability distributions, we formulate a rectangular uncertainty set and, subsequently, the associated chance constraints. Second, assuming a Gaussian distribution of the forecast errors, we provide an analytical reformulation of the chance constraints. Corrective control policies for active power, reactive power, and voltage are included in the formulation.

B. Convex Relaxations of Optimal Power Flow Problem and Relaxation Gap

In general, the AC-OPF is a non-convex, non-linear problem. As a result, identified solutions are not guaranteed to be globally optimal and the distance to the global optimum cannot be specified. Recent advancements in the area of convex optimization with polynomials have achieved to relax the non-linear, non-convex optimal power flow problem and transform it to a convex semidefinite (SDP) or second-order cone problem [15]–[17]. The solution to the convex relaxation is always a lower bound to the global optimum of the original non-convex problem. The term relaxation gap denotes the difference between the minimum obtained through the convex relaxation and the global minimum of the original non-convex problem. A relaxation is tight, if the relaxation gap is small. A relaxation is exact, if the relaxation gap is zero. Zero relaxation gap is achieved when the minimum of the convex relaxation coincides with the global minimum of the original non-convex, non-linear problem. Since the work in [18] has shown cases in which the semidefinite relaxation of [15] fails, it is necessary to investigate the relaxation gap of the obtained solution,

and examine the conditions under which we can obtain zero relaxation gap. In the work [19] a reactive power penalty is introduced, which allows to upper bound the distance to global optimum. In this work, we develop a penalized semidefinite formulation for a chance constrained AC-OPF, which allows us as well to determine an upper bound of the distance to the global optimum. In Fig. 1 we illustrate the previously explained concepts in the context of our work. With relaxation gap, we refer to the gap between the semidefinite relaxation and a non-linear chance constrained AC-OPF which uses the affine policy to parametrize the solution space.

Formulating a convex optimization problem results in tractable solution algorithms that can determine the global minimum. Within power systems, finding the global minimum has two important implications. First, from an economic point of view, it can result to substantial cost savings. Even if the relative difference between a local and the global minimum of a cost minimizing OPF is small, this can still reflect tens to hundreds of millions of dollars in absolute numbers [20]. Second, from a technical point of view the global optimum determines a lower or an upper bound of the required control effort. This can be especially helpful in branch-and-bound methods for mixed integer formulations (e.g. unit commitment, or capacitor switching), as it can be more effective in appropriately “pruning” the search space.

C. Main Contributions

In this work we propose a framework for a convex chance-constrained AC-OPF. The work in [21] makes a first step towards such a formulation which takes into account security related constraints and uncertainty. The change of the system state is described with an affine policy as an explicit function of the forecast errors. A combination of the scenario approach and robust optimization is used to ensure tractability of the chance constraints [22]. For the convex relaxations we build upon the SDP AC-OPF formulation proposed in [15]. The contributions of our work are the following:

- To the best of our knowledge, this is the first paper that proposes a convex formulation for the chance-constrained OPF that (a) is able to determine if it has found the global minimum of the original non-convex problem¹, and (b) if not, it is able to determine the distance to the global minimum through the relaxation gap. As discussed earlier, existing approaches that define convex chance-constrained problems can be divided in two large categories: either they limit themselves to DC-OPF only which is a significant approximation of the original power flow equations neglecting losses, reactive power and voltage, e.g. [2] and [3]; or they linearize the AC power flow equations around an operating point, e.g. [8]. Although both approaches are convex and have merits, they cannot determine if they have found the global minimum of the original problem.
- Besides introducing a penalty factor on power losses which allows us to obtain near-global optimality guar-

¹As we will discuss later in this paper, in cases where a penalized SDP formulation is necessary, this point corresponds to a near-global minimum.

antees, in this paper we also investigate the conditions under which we can obtain a zero relaxation gap. We show that this penalty term is small in practice, leading to tight near-global optimality guarantees of the obtained solution.

- Extending [21], we include in a convex chance-constrained OPF context both an explicit representation with constraints for all relevant power system variables, including active and reactive power, voltage magnitudes, and voltage angles, as well as corrective control strategies. More specifically, our formulation allows to determine corrective control policies which adjust not only the active power but also voltage set-points of generators and reactive power set-points of wind farms as a function of the forecast errors. The proposed framework can be extended to include general corrective control policies related to active and reactive power and voltage.
- As far as the chance constraints are concerned, we use a piecewise affine policy, extending further the work proposed in [21]. Instead of linearizing around the operating point as in [11], [12] and then extrapolating to determine the change in voltage as a linear function of the uncertain injections, in this paper we explicitly consider the nonlinearities at both the current operating point and the worst realization of the uncertainty; subsequently, we perform a linear interpolation between the two points. This improves significantly the accuracy of our method.
- We formulate tractable chance constraints suitable for semidefinite programming for two types of uncertainty sets. First, using a piecewise affine policy, we state a tractable formulation of the chance constrained AC-OPF with convex relaxations that makes no prior assumptions on the type of probability distribution. Using existing data or scenarios, we determine a rectangular uncertainty set; as the set and the chance constraints are affine or convex, we can account for the whole set by enforcing the chance constraints only at its vertices [22]. Second, assuming Gaussian distributions, we formulate tractable chance constraints for the optimal power flow equations that are suitable for semidefinite programming. In that, we also assume the correlation of different uncertain variables. To the best of our knowledge, this is the first paper that introduces a tractable reformulation of the chance-constrained AC-OPF with convex relaxations for Gaussian distributions.
- Based on realistic forecast data and an IEEE 118 bus test case, we compare our approach for both uncertainty sets to the chance constrained DC-OPF formulation in [5], and the iterative AC-OPF in [12]. Compared to the DC-OPF formulation, we find that the formulations proposed in this paper are more accurate and significantly decrease constraint violations. For the rectangular uncertainty set, the affine policy complies with all considered chance constraints and outperforms all other methods having the lowest number of constraint violations. At the same time, we obtain tight near-global optimality guarantees which ensure that the distance to the global optimum is smaller than 0.01% of the objective value. For a Gaussian

TABLE I
NOMENCLATURE

$\mathcal{N}, \mathcal{L}, \mathcal{G}$	Set of buses, lines and generators in the power network
c_{k2}, c_{k1}, c_{k0}	Quadratic, linear and constant cost of generator k
P_{Gk}, Q_{Gk}	Active and reactive power generation at bus k
V_k	Voltage magnitude at bus k
P_{lm}, S_{lm}	Active and apparent branch flow on line (l, m)
Y	Admittance matrix
e_k	k -th basis vector
\bar{y}_{lm}, y_{lm}	Shunt and series admittance of line (l, m)
\mathbf{V}	Complex bus voltage vector
\mathbf{X}	Real and imaginary bus voltage vector
P_{Dk}, Q_{Dk}	Active and reactive power consumption at bus k
n_b	Number of buses in the power network
W	Matrix with product of voltages
n_W	Number of wind farms
\mathcal{W}	Set of buses with wind farms
P_W	Wind infeed
P_W^f	Forecasted wind infeed
ζ	Wind forecast error
ϵ	Maximum violation probability of chance constraints
$W(\zeta_i)$	System matrix as a function of the forecast errors
W_0	Solution for forecasted system state
B_i	Voltage change for forecast error i
B_i^u	Voltage change for upper limit on forecast error i
B_i^l	Voltage change for lower limit on forecast error i
d_G	Generator participation factors
d_W	Wind deviation vector
γ	Slack variable on generator participation factor
μ	Weight for power loss penalty
$\cos(\phi)$	Power factor of wind farms
τ	Ratio of maximum reactive to active power
v	Vertices of rectangular uncertainty set
\mathcal{V}	Set of vertices v
\tilde{W}_v	Solution matrix for vertex v
ζ_v	Forecast error for vertex v of uncertainty set
n_v	Number of vertices v
Φ^{-1}	Inverse Gaussian function
κ	Limit on Gaussian forecast error
PTDF_{lm}	Power Transfer Distribution Factor for line (l, m)
x_{lm}	Reactance for line (l, m)
B_{AC}	DC admittance matrix
ρ	Ratio of second to third eigenvalue of W
δ_{opt}	Near-global optimality measure
N_s	Number of scenarios
e	Euler number
β	Confidence parameter
Λ	Covariance matrix
λ, η	Eigenvalues and eigenvectors of covariance matrix

distribution, both the iterative AC-OPF and our approach satisfy the constraint violation limit, with our approach achieving slightly lower costs due to the corrective control capabilities. As the realistic forecast data we used do not follow a Gaussian distribution, we also observed that both approaches may exceed the constraint violation limit at certain timesteps for that dataset.

The remainder of this work is structured as follows: In Section II the convex relaxation of the chance constrained AC-OPF problem is formulated. Section III introduces the piecewise affine policy. Section IV states the linearization based on power transfer distribution factors (PTDFs) which serves as benchmark. Section V investigates the relaxation gap and presents numerical results for a modified IEEE 9 and 118 bus system with two wind farms. Section VI concludes the paper.

The nomenclature is provided in Table I. An underline and

overline denote, respectively, the upper and lower bound of a variable.

II. OPTIMAL POWER FLOW FORMULATION

A. Convex Relaxation of AC Optimal Power Flow

For completeness, we outline the semidefinite relaxation of the AC-OPF problem as formulated in [15]. A power grid consists of \mathcal{N} buses and \mathcal{L} lines. The set of buses with a generator connected is denoted with \mathcal{G} . The following auxiliary variables are introduced for each bus $k \in \mathcal{N}$ and line $(l, m) \in \mathcal{L}$:

$$Y_k := e_k e_k^T Y \quad (1)$$

$$Y_{lm} := (\bar{y}_{lm} + y_{lm}) e_l e_l^T - (y_{lm}) e_l e_m^T \quad (2)$$

$$\mathbf{Y}_k := \frac{1}{2} \begin{bmatrix} \Re\{Y_k + Y_k^T\} & \Im\{Y_k^T - Y_k\} \\ \Im\{Y_k - Y_k^T\} & \Re\{Y_k + Y_k^T\} \end{bmatrix} \quad (3)$$

$$\mathbf{Y}_{lm} := \frac{1}{2} \begin{bmatrix} \Re\{Y_{lm} + Y_{lm}^T\} & \Im\{Y_{lm}^T - Y_{lm}\} \\ \Im\{Y_{lm} - Y_{lm}^T\} & \Re\{Y_{lm} + Y_{lm}^T\} \end{bmatrix} \quad (4)$$

$$\bar{\mathbf{Y}}_k := \frac{-1}{2} \begin{bmatrix} \Im\{Y_k + Y_k^T\} & \Re\{Y_k - Y_k^T\} \\ \Re\{Y_k^T - Y_k\} & \Im\{Y_k + Y_k^T\} \end{bmatrix} \quad (5)$$

$$M_k := \begin{bmatrix} e_k e_k^T & 0 \\ 0 & e_k e_k^T \end{bmatrix} \quad (6)$$

$$\mathbf{X} := [\Re\{\mathbf{V}\} \Im\{\mathbf{V}\}]^T \quad (7)$$

Matrix Y denotes the bus admittance matrix of the power grid, e_k the k -th basis vector, \bar{y}_{lm} the shunt admittance of line $(l, m) \in \mathcal{L}$, y_{lm} the series admittance and \mathbf{V} the vector of complex bus voltages. The non-linear AC-OPF problem can be written using (1) – (7) as

$$\min \sum_{k \in \mathcal{G}} \{c_{k2}(\text{Tr}\{\mathbf{Y}_k W\} + P_{D_k})^2 + c_{k1}(\text{Tr}\{\mathbf{Y}_k W\} + P_{D_k}) + c_{k0}\} \quad (8)$$

subject to the following constraints for each bus $k \in \mathcal{N}$ and line $(l, m) \in \mathcal{L}$:

$$\underline{P}_{G_k} - P_{D_k} \leq \text{Tr}\{\mathbf{Y}_k W\} \leq \bar{P}_{G_k} - P_{D_k} \quad (9)$$

$$\underline{Q}_{G_k} - Q_{D_k} \leq \text{Tr}\{\bar{\mathbf{Y}}_k W\} \leq \bar{Q}_{G_k} - Q_{D_k} \quad (10)$$

$$\underline{V}_k^2 \leq \text{Tr}\{M_k W\} \leq \bar{V}_k^2 \quad (11)$$

$$-\bar{P}_{lm} \leq \text{Tr}\{\mathbf{Y}_{lm} W\} \leq \bar{P}_{lm} \quad (12)$$

$$\text{Tr}\{\mathbf{Y}_{lm} W\}^2 + \text{Tr}\{\bar{\mathbf{Y}}_{lm} W\}^2 \leq \bar{S}_{lm}^2 \quad (13)$$

$$W = \mathbf{X}\mathbf{X}^T \quad (14)$$

The objective (8) minimizes generation cost, where c_{k2} , c_{k1} and c_{k0} are quadratic, linear and constant cost variables associated with power production of generator $k \in \mathcal{G}$. The terms P_{D_k} and Q_{D_k} denote the active and reactive power consumption at bus k . Constraints (9) and (10) include the nodal active and reactive power flow balances; \underline{P}_{G_k} , \bar{P}_{G_k} , \underline{Q}_{G_k} and \bar{Q}_{G_k} are generator limits for minimum and maximum active and reactive power, respectively. The bus voltages are constrained by (11) with corresponding lower and upper limits \underline{V}_k , \bar{V}_k . The active and apparent power branch flow P_{lm} and S_{lm} on line $(l, m) \in \mathcal{L}$ are limited by \bar{P}_{lm} (12) and \bar{S}_{lm} (13), respectively. To obtain an optimization problem linear

in W , the objective function is reformulated using Schur's complement:

$$\min \sum_{k \in \mathcal{G}} \alpha_k \quad (15)$$

$$\begin{bmatrix} c_{k1} \text{Tr}\{\mathbf{Y}_k W\} + a_k & \sqrt{c_{k2}} \text{Tr}\{\mathbf{Y}_k W\} + b_k \\ \sqrt{c_{k2}} \text{Tr}\{\mathbf{Y}_k W\} + b_k & -1 \end{bmatrix} \preceq 0 \quad (16)$$

where $a_k := -\alpha_k + c_{k0} + c_{k1} P_{D_k}$ and $b_k := \sqrt{c_{k2}} P_{D_k}$. In addition, the apparent branch flow constraint (13) is rewritten:

$$\begin{bmatrix} -(\bar{S}_{lm})^2 & \text{Tr}\{\mathbf{Y}_{lm} W\} & \text{Tr}\{\bar{\mathbf{Y}}_{lm} W\} \\ \text{Tr}\{\mathbf{Y}_{lm} W\} & -1 & 0 \\ \text{Tr}\{\bar{\mathbf{Y}}_{lm} W\} & 0 & -1 \end{bmatrix} \preceq 0 \quad (17)$$

The non-convex rank constraint (14) can be expressed by:

$$W \succeq 0 \quad (18)$$

$$\text{rank}(W) = 1 \quad (19)$$

The convex relaxation is introduced by dropping the rank constraint (19), relaxing the non-linear, non-convex AC-OPF to a convex semidefinite program (SDP). The work in [15] proves that if the rank of W obtained from the SDP relaxation is 1, then W is the global optimum of the non-linear, non-convex AC-OPF and the optimal voltage vector can be computed following the procedure described in [23].

B. Inclusion of Chance Constraints

Renewable energy sources and stochastic loads introduce uncertainty in power system operation. To account for uncertainty in bus power injections, we extend the presented OPF formulation with chance constraints. A number of n_W wind farms are introduced in the power grid at buses $k \in \mathcal{W}$ and modeled as

$$P_{W_k} = P_{W_k}^f + \zeta_k \quad (20)$$

where P_{W_k} are the actual wind infeeds, $P_{W_k}^f$ are the forecasted values and ζ are the uncertain forecast errors. To simplify notation, the resulting upper and lower bounds on net active and reactive power injections are written in compact form as:

$$\bar{P}_k := \bar{P}_{G_k} - P_{D_k} + P_{W_k}^f + \zeta_k, \quad (21)$$

$$\underline{P}_k := \underline{P}_{G_k} - P_{D_k} + P_{W_k}^f + \zeta_k \quad (22)$$

$$\bar{Q}_k := \bar{Q}_{G_k} - Q_{D_k} \quad (23)$$

$$\underline{Q}_k := \underline{Q}_{G_k} - Q_{D_k} \quad (24)$$

The convex chance constrained AC-OPF problem includes chance constraints for each bus $k \in \mathcal{N}$ and line $(l, m) \in \mathcal{L}$:

$$\min \sum_{k \in \mathcal{G}} \alpha_k \quad (25)$$

$$\text{s.t. (9), (10), (11), (12), (17), (16), (18) for } W = W_0 \quad (26)$$

$$\mathbb{P}\left\{P_k \leq \text{Tr}\{\mathbf{Y}_k W(\zeta)\} \leq \bar{P}_k, \quad (27)$$

$$Q_k \leq \text{Tr}\{\bar{\mathbf{Y}}_k W(\zeta)\} \leq \bar{Q}_k, \quad (28)$$

$$V_k^2 \leq \text{Tr}\{M_k W(\zeta)\} \leq \bar{V}_k^2, \quad (29)$$

$$-\bar{P}_{lm} \leq \text{Tr}\{\mathbf{Y}_{lm} W(\zeta)\} \leq \bar{P}_{lm}, \quad (30)$$

$$\begin{bmatrix} -(\bar{S}_{lm})^2 & \text{Tr}\{\mathbf{Y}_{lm} W(\zeta)\} & \text{Tr}\{\bar{\mathbf{Y}}_{lm} W(\zeta)\} \\ \text{Tr}\{\mathbf{Y}_{lm} W(\zeta)\} & -1 & 0 \\ \text{Tr}\{\bar{\mathbf{Y}}_{lm} W(\zeta)\} & 0 & -1 \end{bmatrix} \preceq 0, \quad (31)$$

$$W(\zeta) \succeq 0 \Big\} \geq 1 - \epsilon \quad (32)$$

The parameter $\epsilon \in (0, 1)$ defines the upper bound on the violation probability of the chance constraints (27) – (32). The function $W(\zeta)$ denotes the system state as a function of the forecast errors. The chance constrained AC-OPF problem (25) – (32) is an infinite-dimensional problem optimizing over $W(\zeta)$ which is a function of a continuous uncertain variable ζ [21]. This renders the problem intractable, which makes it necessary to identify a suitable approximation for $W(\zeta)$ [24]. In the following, an approximation of an explicit dependence of $W(\zeta)$ on the forecast errors is presented.

III. AFFINE POLICY

We present a formulation of the chance constraints using an affine policy, which approximates the system change as a linear function of the forecast errors. This allows us to include corrective control policies for active and reactive power, and voltages. We propose a tractable formulation for two types of uncertainty sets. First, using an approach based on randomized and robust optimization, and making no prior assumption on the underlying probability distributions, we determine a rectangular uncertainty set. For that, it is sufficient to enforce the chance constraints at its vertices. Second, assuming a Gaussian distribution of the forecast errors, we can provide an analytical reformulation of the linear chance constraints and a suitable approximation of the semidefinite chance constraints.

A. Formulation of Chance Constraints

The main idea is to describe the matrix $W(\zeta)$ as the sum of the forecasted system operating state W_0 and the change of the system state B_i due to each forecast error. Similar to [21], the matrix $W(\zeta)$ is approximated using the affine policy

$$W(\zeta) = W_0 + \sum_{i=1}^{n_w} \zeta_i B_i \quad (33)$$

where W_0 and B_i are matrices modeled as decision variables. Eq. (33) provides an affine parametrization of the solution space for the product of real and imaginary part of bus voltages described by $W(\zeta)$. The main advantages of the affine policy are that it resembles an affine corrective control policy and naturally allows to include these. Furthermore, as the

system change depends linearly on the forecast error, in case a Gaussian distribution is assumed, an analytical reformulation can be applied. Inserting (33) in (27) – (32) yields:

$$\mathbb{P}\left\{P_k \leq \text{Tr}\{\mathbf{Y}_k W_0\} + \sum_{i=1}^{n_w} \zeta_i \text{Tr}\{\mathbf{Y}_k B_i\} \leq \bar{P}_k \quad (34)$$

$$Q_k \leq \text{Tr}\{\bar{\mathbf{Y}}_k W_0\} + \sum_{i=1}^{n_w} \zeta_i \text{Tr}\{\bar{\mathbf{Y}}_k B_i\} \leq \bar{Q}_k \quad (35)$$

$$V_k^2 \leq \text{Tr}\{M_k W_0\} + \sum_{i=1}^{n_w} \zeta_i \text{Tr}\{M_k B_i\} \leq \bar{V}_k^2 \quad (36)$$

$$-\bar{P}_{lm} \leq \text{Tr}\{\mathbf{Y}_{lm} W_0\} + \sum_{i=1}^{n_w} \zeta_i \text{Tr}\{\mathbf{Y}_{lm} B_i\} \leq \bar{P}_{lm} \quad (37)$$

$$\begin{bmatrix} -\bar{S}_{lm}^2 & \Xi_{lm}^P & \Xi_{lm}^Q \\ \Xi_{lm}^P & -1 & 0 \\ \Xi_{lm}^Q & 0 & -1 \end{bmatrix} \preceq 0 \quad (38)$$

$$W_0 + \sum_{i=1}^{n_w} \zeta_i B_i \succeq 0 \Big\} \geq 1 - \epsilon \quad (39)$$

The terms $\Xi_{lm}^P := \text{Tr}\{\mathbf{Y}_{lm} W_0\} + \sum_{i=1}^{n_w} \zeta_i \text{Tr}\{\mathbf{Y}_{lm} B_i\}$ and $\Xi_{lm}^Q := \text{Tr}\{\bar{\mathbf{Y}}_{lm} W_0\} + \sum_{i=1}^{n_w} \zeta_i \text{Tr}\{\bar{\mathbf{Y}}_{lm} B_i\}$ denote the active and reactive power flow on transmission line $(l, m) \in \mathcal{L}$ as a function of the forecast errors. Note that the chance constraints (34) – (39) are convex and can be classified in two groups: The constraints (34) – (37) are linear scalar chance constraints and the constraints (38) – (39) are semidefinite chance constraints.

B. Corrective Control Policies

The affine policy allows to include corrective control policies related to active power, reactive power, and voltage in the AC-OPF formulation. In this work, the implemented policies are generator active power control, generator voltage control, and wind farm reactive power control.

Throughout the transmission system, generation has to match demand and system losses. If an imbalance occurs, automatic generation control (AGC) restores the system balance [25]. Hence, designated generators in the power grid will respond to changes in wind power by adjusting their output as part of secondary frequency control. The generator participation factors are defined in the vector $d_G^i \in \mathbb{R}^{n_b}$ for each wind infeed $i \in \{1, n_w\}$. The term n_b denotes the number of buses. The sum of the change in generator active power set-points should compensate the deviation in wind generation, i. e. $\sum_{k \in \mathcal{G}} d_{G_k}^i = 1$. The wind vector $d_{W_k}^i \in \mathbb{R}^{n_b}$ has a $\{-1\}$ entry corresponding to the bus where the i -th wind farm is located at. The other entries are zero. The line losses of the AC power grid vary non-linearly with changes in wind infeeds. To compensate for this change in system losses, we add a slack variable γ_i to the generator set-points. This results in the following constraints on each matrix B_i for each bus k in \mathcal{N} and each wind feed-in i in $\{1, n_w\}$:

$$\text{Tr}\{\mathbf{Y}_k B_i\} = d_{G_k}^i (1 + \gamma_i) + d_{W_k}^i \quad (40)$$

As a result of (40), it is ensured that each generator equally compensates the change in system losses according to its participation factor. To constrain the magnitude of the slack

variable, a penalty term is added to the objective function (25), where the term $\mu \geq 0$ is a weighting factor:

$$\min \sum_{k \in \mathcal{G}} \alpha_k + \mu \sum_i^{n_w} \gamma_i \quad (41)$$

This penalty guides the optimization to a physically meaningful solution, i.e. it allows us to obtain rank-1 solution matrices. The increase in losses due to deviations in wind infeeds is minimized. With this penalized semidefinite AC-OPF formulation, near-global optimality guarantees can be derived specifying the maximum distance to the global optimum [19]. The numerical results show that while this penalty is necessary to obtain zero relaxation gap, in practice the deviation from the global optimum is very small. This is investigated in detail in the results section.

In power systems, automatic voltage regulators (AVR) are installed as part of the control unit of generators. They keep the voltages at the generator terminals to a value fixed by the operator or a higher level controller [26]. The voltage set-point at each generator $k \in \mathcal{G}$ is changed as a function of the forecast errors [21] and can be retrieved using:

$$V_k(\zeta)^2 = \text{Tr}\{M_k W_0\} + \sum_{i=1}^{n_w} \zeta_i \text{Tr}\{M_k B_i\} \quad (42)$$

According to recent revisions in Grid Codes [27], renewable generators such as wind farms have to be able to provide or absorb reactive power up to a certain extent. This is often specified in terms of a power factor $\cos \phi := \sqrt{\frac{P^2}{P^2 + Q^2}}$. In this paper, we include the reactive power capabilities of the wind farms in the optimization. Note that these vary depending on the magnitude of the actual wind infeed. For each $k \in \mathcal{W}$ the constraints (23) and (24) are replaced by:

$$\overline{Q}_k := \overline{Q}_{G_k} - Q_{D_k} + \tau(P_{W_k}^f + \zeta_k) \quad (43)$$

$$\underline{Q}_k := \underline{Q}_{G_k} - Q_{D_k} - \tau(P_{W_k}^f + \zeta_k) \quad (44)$$

where $\tau := \sqrt{\frac{1 - \cos^2 \phi}{\cos^2 \phi}}$. Using this procedure, active and reactive power set-points of FACTS devices and HVDC converter can also be included in the optimization.

C. Piecewise Affine Policy

In Fig. 2 the affine policy for a wind infeed P_{W_i} is depicted. By choosing an affine policy in the form of (33), the maximum and minimum bounds of the uncertainty set are linearly connected using the matrix B_i , and the OPF solution at the bounds can be recovered. As the OPF is a non-linear problem, the true system variation will likely not coincide with the linearization. Hence, the affine policy of [21] is not exact at the operating point W_0 , but returns only an estimate W'_0 , i.e. a non-physical higher rank solution. To obtain an exact solution for W_0 , i.e. a rank-1 solution, we introduce a modification to the conventional affine policy by separating the linearization between the maximum and minimum value into an upper part B_i^u and a lower part B_i^l , and thereby introducing a piecewise affine policy. Thus, we linearize between the operating point and the maximum and minimum value of the uncertainty set,

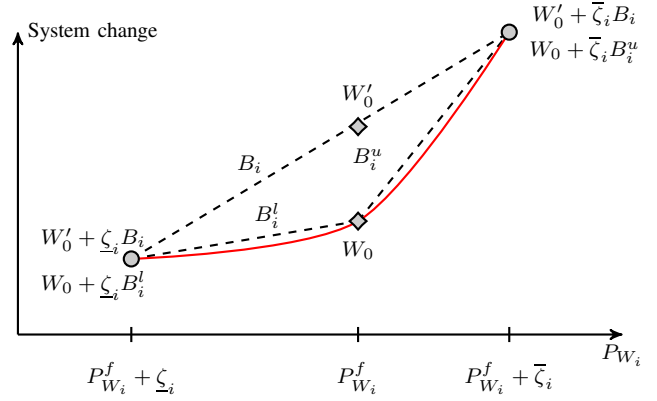


Fig. 2. Piecewise affine policy: The linearization between upper and lower limit is split into two corresponding piecewise linearizations starting from the exact operating point W_0 . The red line indicates the true system behavior and the dashed lines the approximation which is made with the corresponding affine policy. This modification allows us to obtain the exact rank-1 solution W_0 , not the higher-rank approximation W'_0 .

respectively. We extend the work of [21], by ensuring that the obtained solution is exact at the operating point. An additional benefit of our approach is that we get a closer approximation of the true system behavior, while the obtained control policies are piecewise linear.

D. Tractable Formulation for Rectangular Uncertainty Set

In this section, we provide a tractable formulation of the chance constraints for a rectangular uncertainty set. The proposed procedure is a combination of robust and randomized optimization from [22] and applied in [21]. A scenario-based method, which does not make any assumption on the underlying distribution of the forecast errors, is used to compute the bounds of the uncertainty set. Two parameters need to be specified, $\epsilon \in (0, 1)$ is the allowable violation probability of the chance constraints and $\beta \in (0, 1)$ a confidence parameter. Then, the minimum volume hyper-rectangular set is computed, which with probability $1 - \beta$ contains $1 - \epsilon$ of the probability mass. According to [21], it is necessary to include at least the following number of scenarios N_s to specify the uncertainty set:

$$N_s \geq \frac{1}{1 - \epsilon} \frac{e}{e - 1} \left(\ln \frac{1}{\beta} + 2n_w - 1 \right) \quad (45)$$

The term e is Euler's number. The minimum and maximum bounds on the forecast errors $\zeta_i \in [\underline{\zeta}_i, \bar{\zeta}_i]$ are retrieved by a simple sorting operation among the N_s scenarios and the vertices of the rectangular uncertainty set can be defined. With the term vertices we denote the corner points of the rectangular uncertainty set.

To obtain a tractable formulation of the chance constraints, the following result from robust optimization is used: If the constraint functions are linear, monotone or convex with respect to the uncertain variables, then the system variables will only take the maximum values at the vertices of the uncertainty set [22]. The chance constraints (34) – (37) in the optimization problem are linear and the semidefinite chance constraints (38), (39) are convex. Hence, it suffices to enforce

the chance constraints at the vertices $v \in \mathcal{V}$ of the uncertainty set.

The vector ζ_v collects the forecast error magnitudes for each vertex. The generator participation factors $d_{G_k}^v$, wind vector $d_{W_k}^v$, as well as the corresponding slack variable γ_v are defined for each vertex. To obtain a compact formulation, we introduce the following auxiliary variable:

$$W_v := W_0 + \sum_{i=1}^{n_W} \zeta_{v_i} B_i \quad (46)$$

The matrix W_v denotes the power flow solution at the corresponding vertex v . The active and reactive power limits for each bus $k \in \mathcal{N}$ and vertex $v \in \mathcal{V}$ can be written as:

$$\overline{Q}_k^v := \overline{Q}_{G_k} - Q_{D_k} + \tau(P_{W_k}^f + \zeta_{v_k}) \quad (47)$$

$$\underline{Q}_k^v := \underline{Q}_{G_k} - Q_{D_k} - \tau(P_{W_k}^f + \zeta_{v_k}) \quad (48)$$

$$\overline{P}_k^v := \overline{P}_{G_k} - P_{D_k} + P_{W_k}^f + \zeta_v \quad (49)$$

$$\underline{P}_k^v := \underline{P}_{G_k} - P_{D_k} + P_{W_k}^f + \zeta_v \quad (50)$$

We provide a tractable formulation of chance constraints (34) – (39) for each vertex $v \in \mathcal{V}$, bus $k \in \mathcal{N}$ and line $(l, m) \in \mathcal{L}$:

$$\underline{P}_k^v \leq \text{Tr}\{\mathbf{Y}_k W_v\} \leq \overline{P}_k^v \quad (51)$$

$$\underline{Q}_k^v \leq \text{Tr}\{\tilde{\mathbf{Y}}_k W_v\} \leq \overline{Q}_k^v \quad (52)$$

$$\underline{V}_k^2 \leq \text{Tr}\{M_k W_v\} \leq \overline{V}_k^2 \quad (53)$$

$$-\overline{P}_{lm} \leq \text{Tr}\{\mathbf{Y}_{lm} W_v\} \leq \overline{P}_{lm} \quad (54)$$

$$\begin{bmatrix} -(\overline{S}_{lm})^2 & \text{Tr}\{\mathbf{Y}_{lm} W_v\} & \text{Tr}\{\tilde{\mathbf{Y}}_{lm} W_v\} \\ \text{Tr}\{\mathbf{Y}_{lm} W_v\} & -1 & 0 \\ \text{Tr}\{\tilde{\mathbf{Y}}_{lm} W_v\} & 0 & -1 \end{bmatrix} \preceq 0 \quad (55)$$

$$W_v \succeq 0 \quad (56)$$

$$\text{Tr}\{\mathbf{Y}_k(W_v - W_0)\} = \sum_{i=1}^{n_W} \zeta_{v_i} (d_{G_k}^v (1 + \gamma_v) + d_{W_k}^v) \quad (57)$$

The constraint (57) links the forecasted system state to each of the vertices. To enforce the semidefinite chance constraint (39) for the uncertainty set, it suffices that W_v is positive semidefinite at the vertices of the uncertainty set, e.g. (56) is fulfilled.

Proof. For positive semidefiniteness it must hold $\forall x \in \mathbb{R}^n$:

$$x^T W_v x = x^T (W_0 + \overline{\zeta}_v \tilde{B}_v) x = x^T W_0 x + \overline{\zeta}_v x^T \tilde{B}_v x \geq 0$$

As W_0 is positive semidefinite (18), it follows:

$$x^T W_0 x \geq 0 \Rightarrow -x^T W_0 x \leq \overline{\zeta}_v x^T \tilde{B}_v x$$

Hence, (39) holds at least for $\zeta_i \in [0, \overline{\zeta}_v]$. It follows that by including (56) for each W_v , the solution matrix is semidefinite for the rectangular set. \square

For illustrative purposes, in Fig. 3 a rectangular uncertainty set is depicted for two uncertain wind infeeds P_{W_1} and P_{W_2} . The resulting optimization problem for a rectangular uncertainty set of dimension n_w is minimizing objective (41) subject to constraints (26) and (51) – (57). Note that the proposed formulation holds for an arbitrary high-dimensional rectangular uncertainty set.

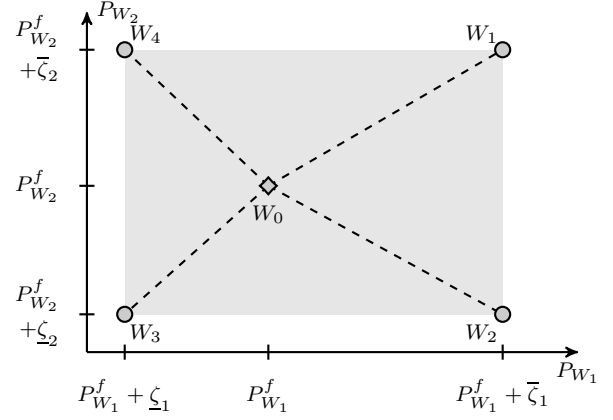


Fig. 3. Rectangular uncertainty set derived from a scenario-based method displayed for two wind farms. It is sufficient to enforce the chance constraints at the vertices of the uncertainty set. The vertices are denoted with circles.

E. Tractable Formulation for Gaussian Uncertainty Set

In the following, it is assumed that the forecast errors ζ are random variables following a Gaussian distribution with zero mean and covariance matrix Λ . We give a direct tractable formulation of the chance constrained AC-OPF, as the work in [3] presented for the chance constrained DC-OPF.

For a defined confidence interval $1 - \epsilon$, the uncertainty set for a Gaussian distribution of the forecast errors is an ellipsoid. First, the direction of linearization of the B matrices is rotated to correspond to the ellipsoid axes which are described by the eigenvectors η_i of the covariance matrix. The eigenvalues λ_i describe the squared dimension of the ellipsoid in the direction of its axes. Similar to the rectangular uncertainty set, we introduce the following auxiliary variables for each wind infeed i in $\{1, n_W\}$ and bus $k \in \mathcal{W}$:

$$\tilde{d}_G^i := d_G \|\eta_i\|, \tilde{d}_{W_k}^i := \eta_i, \tilde{\zeta}_i := \sqrt{\lambda_i} \quad (58)$$

With \tilde{B}_i we denote the matrices of the affine policy rotated in the direction of the ellipsoid axes and constraint (40) has to hold:

$$\text{Tr}\{\mathbf{Y}_k \tilde{B}_i\} = \tilde{d}_{G_k}^i (1 + \gamma_i) + \tilde{d}_{W_k}^i \quad (59)$$

Second, we use theoretical results on chance constraints from the work in [28], which presents the theory for an analytical reformulation of linear scalar chance constraints. To apply the reformulation, we approximate the joint probability of the chance constraint violation (34)–(39) with the violation probability of each individual chance constraint, which is conservative. Applying the reformulation to the chance constraints (34) – (37) yields for each bus $k \in \mathcal{N}$ and line $(l, m) \in \mathcal{L}$:

$$\underline{P}_k \leq \text{Tr}\{\mathbf{Y}_k W_0\} \pm \sqrt{\sum_i^{n_w} \kappa_i^2 \text{Tr}\{\mathbf{Y}_k \tilde{B}_i\}^2} \leq \overline{P}_k \quad (60)$$

$$\underline{Q}_k \leq \text{Tr}\{\tilde{\mathbf{Y}}_k W_0\} \pm \sqrt{\sum_i^{n_w} \kappa_i^2 \text{Tr}\{\tilde{\mathbf{Y}}_k \tilde{B}_i\}^2} \leq \overline{Q}_k \quad (61)$$

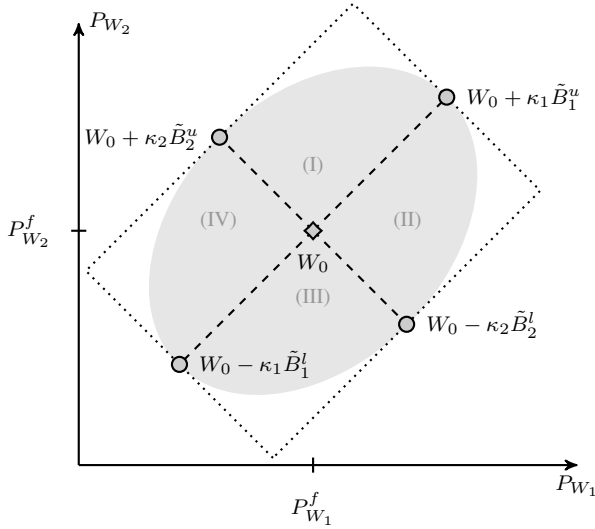


Fig. 4. Uncertainty set resulting from a Gaussian distribution of the forecast errors considering correlation. The directions of approximation for the affine policy are rotated corresponding to the eigenvectors of the covariance matrix. The circles denote the points for which the definite chance constraint is enforced. As a result, it holds for the whole dotted rectangular shape. The indices (I) – (IV) denote the four quadrants of the uncertainty set for each of which the complete set of chance constraints (55) and (60) – (64) is included.

$$\underline{V}_k^2 \leq \text{Tr}\{M_k W_0\} \pm \sqrt{\sum_i^{n_w} \kappa_i^2 \text{Tr}\{M_k \tilde{B}_i\}^2} \leq \overline{V}_k^2 \quad (62)$$

$$-\overline{P}_{lm} \leq \text{Tr}\{\mathbf{Y}_{lm} W_0\} \pm \sqrt{\sum_i^{n_w} \kappa_i^2 \text{Tr}\{\mathbf{Y}_{lm} \tilde{B}_i\}^2} \leq \overline{P}_{lm} \quad (63)$$

The term $\kappa_i := \Phi^{-1}(1-\epsilon)\tilde{\zeta}_i$ is introduced, where Φ^{-1} denotes the inverse Gaussian function. The chance constraint (39) is a linear matrix inequality which ensures that the matrix $W_0 + \sum_i^{n_w} \tilde{\zeta}_i \tilde{B}_i$ is positive semidefinite inside a confidence interval $1 - \epsilon$. An analytical reformulation of this type of constraint is not known [28]. As a safe approximation, it suffices to enforce that $W_0 + \sum_i^{n_w} \tilde{\zeta}_i \tilde{B}_i$ is positive semi-definite at maximum corresponding deviations $\pm\kappa_i$ to ensure that (32) is fulfilled:

$$W_0 \pm \kappa_i \tilde{B}_i \succeq 0 \quad \forall i \in \mathcal{W} \quad (64)$$

This is motivated by the same proof used for (56). This results in (39) holding for the outer rectangular approximation of the ellipsoid uncertainty set. The semidefinite chance constraint on the apparent branch power flow can be conservatively approximated by enforcing it for the smallest rectangular set enclosing the ellipsoid, i.e. by including the constraint (55) in the optimization.

The assumption of a multivariate Gaussian distribution of the forecast errors leads to an uncertainty set which in two dimensions can be described as an ellipse. For the case of two wind farms with uncertain infeeds P_{W_1} and P_{W_2} this configuration is depicted in Fig. 4. Incorporating the results on the modification of the affine policy presented in section III-C, we add the constraints (60) – (63) not for B_i but for both B_i^u and B_i^l and each of their combinations, splitting the uncertainty set into four quadrants (I) – (IV) as depicted

in Fig. 4. The resulting optimization problem corresponds to minimizing objective function (41) subject to constraints (26), (55) and (60) – (64) for each quadrant of the ellipsoid.

IV. LINEARIZATION USING PTDFs

In the following, an alternative approach is presented which is used as benchmark for comparison with the rest of the approaches presented in this paper. To describe the system change as a function of the forecast errors, in this section we introduce a linear approximation based on DC power flow. This linear approximation uses the so-called power transfer distribution factors (PTDFs) to estimate the change in line loading due to a change in active power injections. This approach has been used in the works in [3] and [29] in the context of DC- and AC-OPF, respectively.

The PTDFs use the DC power flow representation, i.e. assuming that the voltage magnitudes of all buses are equal to 1 p.u. and the resistances of branches are neglected. Hence, line losses are neglected and the generator participation factors d_G are defined without including the slack term γ . As we assume constant voltage magnitudes, the semidefinite (32), the voltage (29) and the reactive power (28) chance constraints are dropped and the focus is on approximating the chance constraints for the active power bus injection and active power branch flow, Eqs. (27) and (30). The admittance matrix B_{DC} is constructed using only the line reactances x_{lm} . The resulting matrix is singular. Thus, one column and the corresponding row are removed to obtain \tilde{B}_{DC} . The vectors d_G and d_W collect the generator participation factors and wind injections, and \tilde{d}_G and \tilde{d}_W denote the corresponding vectors with the first entry removed. The PTDF for each line $(l, m) \in \mathcal{L}$ and uncertain wind infeed i is defined as follows:

$$\text{PTDF}_{lm}^i = (e_l - e_m)^T \frac{1}{x_{lm}} \tilde{B}_{DC}^{-1} (\tilde{d}_G^i + \tilde{d}_W^i) \quad (65)$$

The PTDFs provide an approximate linear relation between a change in bus power injections and the change of the active power flow over a transmission line. Assuming the maximum and minimum bounds of the forecast errors are given by $[-\bar{\zeta}_i, \bar{\zeta}_i]$ from e.g. the previously described scenario-based approach, we formulate a tractable approximation of (27) and (30) for each bus $k \in \mathcal{N}$ and line $(l, m) \in \mathcal{L}$:

$$\underline{P}_k^f \leq \text{Tr}\{\mathbf{Y}_k W_0\} \pm \sum_i^{n_w} \bar{\zeta}_i (d_{G_k}^i + d_{W_k}^i) \leq \overline{P}_k^f \quad (66)$$

$$-\overline{P}_{lm} \leq \text{Tr}\{\mathbf{Y}_{lm} W_0\} \pm \sum_i^{n_w} \bar{\zeta}_i \text{PTDF}_{lm}^i \leq \overline{P}_{lm} \quad (67)$$

Assuming the forecast errors follow a Gaussian distribution with zero mean and co-variance matrix Λ , we formulate a tractable approximation of (27) and (30) for each bus $k \in \mathcal{N}$ and line $(l, m) \in \mathcal{L}$:

$$\underline{P}_k^f \leq \text{Tr}\{\mathbf{Y}_k W_0\} \pm \Phi^{-1}(1-\epsilon) \sqrt{d_{G_k}^T \Lambda d_{G_k}} \leq \overline{P}_k^f \quad (68)$$

$$-\overline{P}_{lm} \leq \text{Tr}\{\mathbf{Y}_{lm} W_0\} \pm \Phi^{-1}(1-\epsilon) \sqrt{\text{PTDF}_{lm}^T \Lambda \text{PTDF}_{lm}} \leq \overline{P}_{lm} \quad (69)$$

V. SIMULATION AND RESULTS

In this section, we describe first the simulation setup. Subsequently, in order to provide a better overview of our results we use the IEEE 24-bus test case. There, we investigate the relaxation gap of the obtained solution matrices as a function of the penalty weight. Detailed results on an IEEE 9 and a 118-bus test case are provided in the next section.

A. Simulation Setup

The optimization problem is implemented in Julia using the optimization toolbox JuMP [30] and the SDP solver MOSEK 8 [31]. A small resistance of 10^{-4} has to be added to each transformer, which is a condition for obtaining zero relaxation gap [15]. To investigate whether the relaxation gap of an obtained solution matrix W is zero, the ratio ρ of the 2nd to 3rd eigenvalue is computed, a measure proposed by [23]. This value should be around 10^5 or larger for zero relaxation gap to hold, which means that the obtained solution matrix is rank-2. The respective rank-1 solution can be retrieved by following the procedure described in [23]. According to [15], the obtained solution is then a feasible solution to the original non-linear AC-OPF problem.

The work in [19] proposes the use of the following measure to evaluate the degree of the near-global optimality of a penalized SDP relaxation. Let $\hat{f}_1(x)$ be the generation cost of the convex OPF without a penalty term and $\hat{f}_2(x)$ the generation cost of the convex OPF with a penalty weight sufficiently high to obtain rank-1 solution matrices. Then, the near-global optimality can be assessed by computing the parameter $\delta_{\text{opt}} := \frac{\hat{f}_1(x)}{\hat{f}_2(x)} \cdot 100\%$. The closer this parameter is to 100%, the closer the solution is to the global optimum. Note that this distance is an upper bound to the distance from global optimality.

B. Investigating the relaxation gap

This section investigates the relaxation gap of the obtained matrices. With relaxation gap, we refer to the gap between the SDP relaxation and a non-linear chance constrained AC-OPF which uses the affine policy to parametrize the solution space. The IEEE 24 bus system with parameters specified in [32] is used. The allowable violation probability is selected to be $\epsilon = 5\%$. Two wind farms with a forecasted infeed of 50 MW and 150 MW and a maximum power of 150 MW and 400 MW are introduced at buses 8 and 24, respectively. For illustrative purposes, the forecast error for the rectangular uncertainty is assumed to be bounded within $\pm 50\%$ of the forecasted value with 95% probability. For the Gaussian uncertainty set, a standard deviation of 25% of the forecasted value and no correlation between both wind farms is assumed. Each generator adjusts its active power proportional to its maximum active power to react to deviations in wind power output.

For the rectangular uncertainty set, Fig. 5 shows the eigenvalue ratios ρ of the matrices $W_0 - W_4$ as a function of the penalty weight μ . A certain minimum value for the weight $\mu = 175$ is necessary to obtain solution matrices with rank-1, i.e. eigenvalue ratio higher than 10^5 , at the operating state

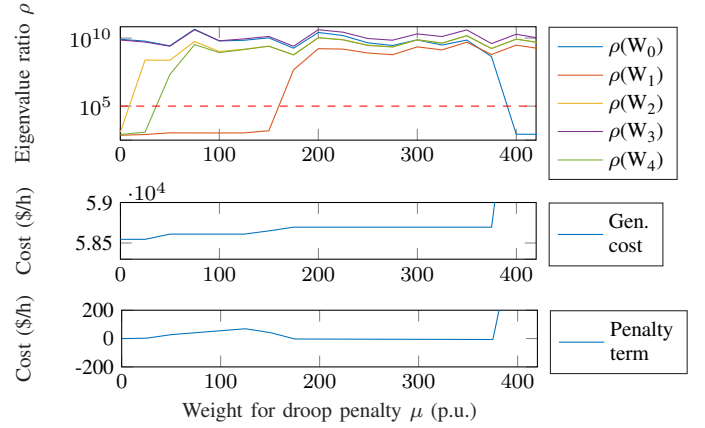


Fig. 5. Eigenvalue ratios ρ , generation cost and penalty term as a function of the power loss penalty weight μ for a IEEE 24 bus test case with two wind farms and a rectangular uncertainty set.

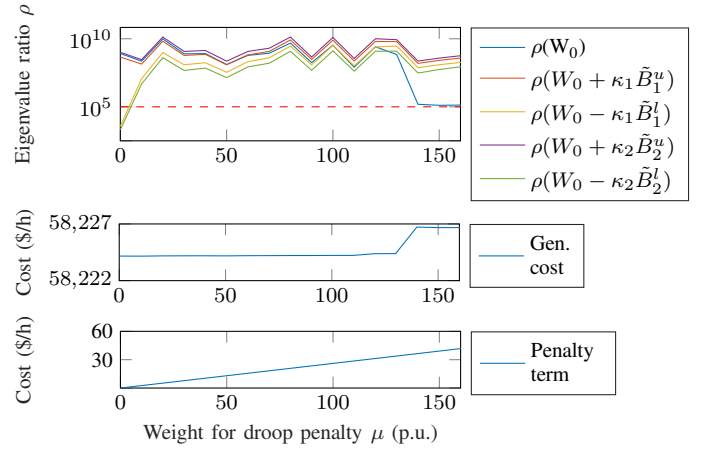


Fig. 6. Eigenvalue ratios ρ , generation cost and penalty term as a function of the power loss penalty weight μ for a IEEE 24 bus test case with two wind farms and a Gaussian uncertainty set.

W_0 and the four vertices of the rectangular uncertainty set $W_1 - W_4$. The near-global optimality at $\mu = 175$ for this test case evaluates to a tight upper bound of 99.74%. If the penalty weight is increased beyond $\mu = 375$ a higher rank solution is obtained for the forecasted system state.

A similar observation can be made if a Gaussian distribution is assumed for the forecast errors. Fig. 6 shows the eigenvalue ratios ρ as a function of the penalty weight μ for the Gaussian uncertainty set. A certain minimum value for the weight $\mu = 10$ is necessary to obtain solution matrices with rank-1 at the operating state W_0 and the four end-point of the ellipsoid axes. The generation cost is almost flat with respect to increasing penalty weight and the near-global optimality at $\mu = 10$ for this test case evaluates to an upper bound larger than 99.99%. The necessary magnitude of the penalty weight μ to obtain rank-1 solution matrices depends on the test case and configuration.

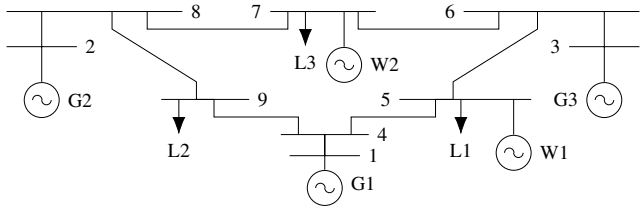


Fig. 7. Modified IEEE 9-bus system with wind farms W1 and W2

C. IEEE 9 bus system

The parameters of the IEEE 9 bus system are provided in [32] which is depicted in Fig. 7. The following modifications are applied: To better illustrate the performance of our methods, we reduce the maximum apparent branch flow, excluding the transformers, by 50% to obtain a more constrained system. As the branch flow constraint is formulated in terms of maximum active power flow, the maximum active branch flow \bar{P}_{lm} is set to 80% of the maximum apparent branch flow \bar{S}_{lm} . The quadratic cost function, limits on voltages, and generator active and reactive power remain unchanged as described in [32]. We add one wind farm with a forecasted infeed $P_{W_1}^f$ of 70 MW at node 5 and a second wind farm with a forecasted infeed $P_{W_2}^f$ of 100 MW at node 7. The wind farms are able to supply a power factor of 0.95 inductive to 0.95 capacitive according to [27]. The three generators equally compensate the deviation in wind power, i.e. their participation factor is $\frac{1}{3}$. The allowable violation ϵ is chosen to be 5%. We choose μ to be 100 p.u. for both test cases.

In the following, we compare the affine policy with the linearization using PTDFs. To evaluate the performance of both approaches, we show the detailed results for the forecasted system state W_0 and the worst-case system state. In the Tables, quantities for the worst-case are denoted with an asterisk $(-)^*$. Furthermore, we evaluate the violation of the constraints for the entire uncertainty set. For this purpose, we evaluate AC power flows for a fine mesh of points inside the uncertainty set. We assume a necessary violation limit of 0.1% to exclude numerical errors. To check if line and voltage constraints are actually violated for the approach using PTDFs, an AC power flow is computed with MATPOWER [32]. As the DC approximation does not account for changes in losses, we distribute this change according to the participation factors. Furthermore, we assume that the approach using PTDFs assigns a fixed power factor $\cos \phi$ to each wind farm. The affine policy includes a generator voltage and wind farm reactive power control, assigning an updated set-point to generators and wind farms based on the actual realization of the forecast errors.

1) Rectangular Uncertainty Set With Two Wind Farms:

In this section, we compare the tractable formulation of the chance constrained AC-OPF for a rectangular uncertainty set with an approach using PTDFs. We assume that from e.g. the scenario approach we obtain upper and lower limits on the forecast errors of both wind farms. The forecast error for the wind farm W1 at node 5 is bounded by $\bar{\zeta}_1 = 35$ MW and for the wind farm W2 at node 7 by $\bar{\zeta}_2 = 60$ MW. Simulations

TABLE II
LINEARIZATION USING PTDFs (RECTANGULAR UNCERTAINTY SET)

Generation cost		$2160.47 \frac{\$}{h}$				
Eigenvalue ratio		$\rho(W_0) = 4.3 \times 10^6$				
Gen #	V_G (p.u.)	P_G (MW)	Q_G (Mvar)	V_G^* (p.u.)	P_G^* (MW)	Q_G^* (Mvar)
G1	1.09	41.67	6.70	1.09	33.88	10.48
G2	1.10	63.02	-6.87	1.10	55.19	-10.98
G3	1.07	42.43	-42.59	1.07	34.60	-45.01
W1	—	70.00	-0.69	—	35.00	-0.34
W2	—	100.00	14.56	—	160.00	23.30
Σ	—	317.12	-28.90	—	318.68	-22.45
Branch	from	to	P_{lm}	P_{lm}^*	\bar{P}_{lm}	
3	5	6	35.38	60.38	60.00	(MW)
Active power losses (MW)			P_{loss}	2.12	P_{loss}^*	3.68
Maximum voltages (p.u.)			V_7^*	1.104	\bar{V}_7	1.100
			V_8^*	1.103	\bar{V}_8	1.100
Branch flow / Voltage violations for uncertainty set						0.1%/37.8%

show that the grid experiences the highest loading if the wind farm W1 produces its minimum power of 35 MW and the wind farm W2 its maximum power of 160 MW.

The results for the PTDF approach are shown in Table II. The generation cost amounts to $2160.47 \frac{\$}{h}$. The eigenvalue ratio $\rho = 4.3 \times 10^6$ is larger than 10^5 and comparison of the SDP results with MATPOWER yields that zero relaxation gap is obtained. For the worst-case scenario, a violation of the line flow constraint from bus 5 to bus 6 by 0.38 MW and a violation of the upper voltage limit of 1.1 p.u. at nodes 7 and 8 is observed. This is due to the model mismatch between the underlying DC power flow approximation used by the PTDFs and the full AC power flow equations. Note that the losses increase by 1.53 MW compared to the forecasted system state W_0 . The additional power flow caused by loss compensation is the main reason for the line overloading. Given that the DC power flow does not account for voltages and reactive power, the overvoltages at nodes 7 and 8 occur. Voltage violations occur on 37.8% of the entire uncertainty set and branch flow violations on 0.1%.

The results of the affine policy are shown in Table III. By using the possibility to adjust the generator voltage and the power factor set-points for both wind farms we observe a slight decrease in the generation cost to $2159.64 \frac{\$}{h}$. The penalty term is $5.37 \frac{\$}{h}$ and significantly smaller than the generation cost. The eigenvalue ratio $\rho = 9.4 \times 10^5$ for the base case W_0 indicates that zero relaxation gap holds. Additionally, for all four vertices of the uncertainty set, we obtain zero relaxation gap. A comparison of the obtained results with MATPOWER AC optimal power flow calculations confirms this finding. The obtained solution for the worst-case scenario shows exact compliance with the branch flow limit of 60.0 MW and the voltage limit of 1.1 p.u. In comparison to the approach using PTDFs, the voltage set-point at node 3 is lowered from 1.07 p.u. to 1.04 p.u. In addition, we observe how the affine policy is able to take into account the varying

TABLE III
AFFINE POLICY (RECTANGULAR UNCERTAINTY SET)

Generation cost	2159.66 $\frac{\$}{h}$					
Penalty term	$\mu \sum_{i=1}^4 \gamma_i = 6.41 \frac{\$}{h}$					
Objective value without penalty	2152.92 $\frac{\$}{h}$					
Near-global optimality guarantee δ_{opt}	99.69%					
Eigenvalue ratios	$\rho(W_0) = 9.4 \times 10^5$ $\rho(W_0 + \bar{\zeta}_1 \bar{B}_1) = 3.9 \times 10^5$ $\rho(W_0 + \bar{\zeta}_2 \bar{B}_2) = 2.0 \times 10^5$ $\rho(W_0 + \bar{\zeta}_3 \bar{B}_3) = 1.5 \times 10^6$ $\rho(W_0 + \bar{\zeta}_4 \bar{B}_4) = 1.5 \times 10^6$					
Gen #	V_G (p.u.)	P_G (MW)	Q_G (Mvar)	V_G^* (p.u.)	P_G^* (MW)	Q_G^* (Mvar)
G1	1.08	40.95	8.57	1.09	33.80	15.10
G2	1.09	63.78	2.08	1.10	54.82	0.69
G3	1.04	42.51	-51.60	1.04	35.20	-56.90
W1	—	70.00	-0.05	—	35.00	-1.57
W2	—	100.00	17.23	—	160.00	24.54
Σ	—	317.24	-23.76	—	318.82	-18.13
Branch	from	to	P_{lm}	P_{lm}^*	\bar{P}_{lm}	
3	5	6	35.37	60.00	60.00	(MW)
Active power losses (MW)			P_{loss}	2.24	P_{loss}^*	3.82
Maximum voltage (p.u.)			V_8^*	1.100	\bar{V}_8	1.100
Branch flow / Voltage violations for uncertainty set						0.0% / 0.0%

reactive power capabilities of both wind farms to achieve compliance with the voltage limits. The proposed formulation leads to a safe operation for the entire uncertainty set. The near-global optimality guarantee evaluates to 99.69%.

2) *Gaussian Uncertainty Set With Two Wind Farms:* In this section, we compare the analytical reformulation and tractable approximation of the chance constrained AC-OPF for a Gaussian uncertainty set with an approach using PTDFs. The standard deviations of the forecast errors are $\sigma_1 = 25$ MW and $\sigma_2 = 40$ MW resulting in a symmetric deviation of $\kappa_1 = 49.0$ MW and $\kappa_2 = 78.4$ MW inside the confidence interval, respectively. To identify the worst-case scenario, the results from the affine policy are used to compute the highest line loading on the border of the ellipse. For this test case this amounts to $P_{W_1} = 25.90$ MW and $P_{W_2} = 134.17$ MW.

In Table IV the results using the PTDFs are shown. The generator cost evaluates to 2161.82 $\frac{\$}{h}$. The eigenvalue ratio is 9.6×10^7 and shows that zero relaxation gap is obtained. For the worst-case scenario, the branch from node 5 to node 6 experiences an overloading by 0.29 MW. Furthermore the upper voltage limit at node 8 is violated. This is a result of the DC approximation used for the PTDFs, which neglects system losses, voltage magnitudes and reactive power. Voltage violations occur on 31.9% of the entire uncertainty set and branch flow violations on 0.3%.

The results for the affine policy are listed in Table V. We obtain zero relaxation gap for the operating point and for the other four circled points in Fig. 4 which correspond to the outer points of the two ellipse axes. For the worst-case scenario, we obtain an eigenvalue ratio of 0.8×10^4 , which is close to zero relaxation gap and near the global optimum. We insert

TABLE IV
LINEARIZATION USING PTDFs (GAUSSIAN UNCERTAINTY SET)

Generation cost	2161.82 $\frac{\$}{h}$					
Eigenvalue ratio	$\rho(W_0) = 9.6 \times 10^7$					
Gen #	V_G (p.u.)	P_G (MW)	Q_G (Mvar)	V_G^* (p.u.)	P_G^* (MW)	Q_G^* (Mvar)
G1	1.08	41.30	8.31	1.08	45.10	15.60
G2	1.10	64.63	0.98	1.10	68.39	5.78
G3	1.04	41.30	-55.47	1.04	45.05	-50.21
W1	—	70.00	-2.13	—	25.90	-0.79
W2	—	100.0	22.94	—	134.17	30.78
Σ	—	317.22	-21.33	—	318.61	1.16
Branch	from	to	P_{lm}	P_{lm}^*	\bar{P}_{lm}	
3	5	6	34.85	60.29	60.00	(MW)
Active power losses (MW)			P_{loss}	2.22	P_{loss}^*	3.61
Maximum voltage (p.u.)			V_8^*	1.102	\bar{V}_8	1.100
Branch flow / Voltage violations for uncertainty set						0.3% / 31.9%

TABLE V
AFFINE POLICY (GAUSSIAN UNCERTAINTY SET)

Generation cost	2160.25 $\frac{\$}{h}$					
Penalty term	$\mu \sum_{i=1}^4 \gamma_i = 2.86 \frac{\$}{h}$					
Objective value without penalty	2159.14 $\frac{\$}{h}$					
Near-global optimality guarantee δ_{opt}	99.95%					
Eigenvalue ratios	$\rho(W_0) = 1.6 \times 10^7$ $\rho(W_0 + \bar{\zeta}_1^u B_1^u) = 5.9 \times 10^6$ $\rho(W_0 + \bar{\zeta}_2^u B_2^u) = 7.5 \times 10^6$ $\rho(W_0 + \bar{\zeta}_1^l B_1^l) = 6.8 \times 10^5$ $\rho(W_0 + \bar{\zeta}_2^l B_2^l) = 4.5 \times 10^6$ $\rho^* = 0.8 \times 10^4$					
Gen #	V_G (p.u.)	P_G (MW)	Q_G (Mvar)	V_G^* (p.u.)	P_G^* (MW)	Q_G^* (Mvar)
G1	1.08	40.95	8.57	1.09	44.83	29.33
G2	1.09	63.78	2.08	1.10	67.68	45.71
G3	1.04	42.51	-51.60	1.00	46.40	-82.15
W1	—	70.00	-0.05	—	25.90	-1.01
W2	—	100.00	17.23	—	134.17	30.10
Σ	—	317.24	-23.76	—	319.38	-0.41
Branch	from	to	P_{lm}	P_{lm}^*	\bar{P}_{lm}	
3	5	6	35.37	59.95	60.00	(MW)
Active power losses (MW)			P_{loss}	2.24	P_{loss}^*	4.28
Maximum voltage (p.u.)			V_8^*	1.094	\bar{V}_8	1.100
Branch flow / Voltage violations for uncertainty set						0.0% / 0.0%

the resulting generator voltage, generator active power and wind farm reactive power set-points of the affine policy in a MATPOWER AC power flow. We observe that the resulting branch flow from node 5 to node 6 is 59.95 MW and below the limit of 60 MW. The upper voltage limit at node 8 is not violated. The resulting generation cost 2160.37 $\frac{\$}{h}$ is slightly lower compared to the approach using PTDFs. The penalty term amounts to 2.84 $\frac{\$}{h}$. The affine policy is safe for the entire Gaussian uncertainty set. The near-global optimality guarantee evaluates to 99.95%. The main difference between

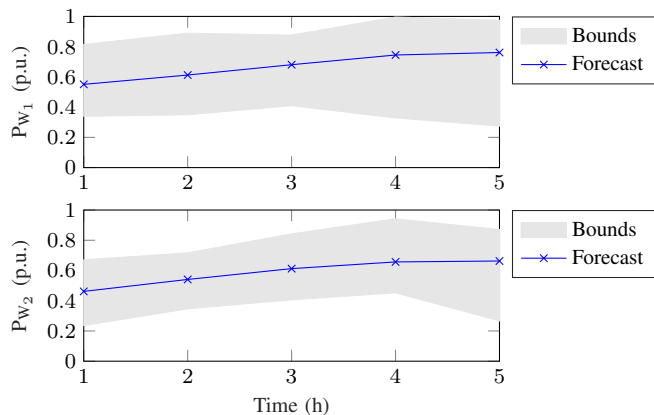


Fig. 8. Forecast data from hour 1 to hour 5. The bounds correspond to the minimum and maximum values from the N_s sampled scenarios for the rectangular uncertainty set.

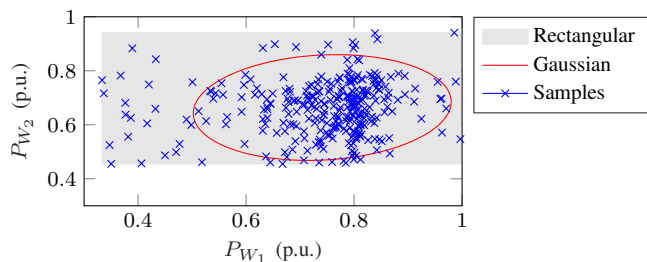


Fig. 9. Comparison of rectangular and Gaussian uncertainty set obtained from the N_s scenarios sampled for hour 4.

both uncertainty sets is the following: For the rectangular set, we obtain a maximum branch flow of 100.0% of the maximum limit, whereas for the Gaussian uncertainty set, we obtain a smaller, conservative value of 99.9% of the maximum limit, which shows that our approximation in (64) is tight.

D. IEEE 118 bus test case

In this section, our proposed approaches using the affine policy and PTDFs are compared with two alternative approaches described in the literature [5], [12]. We use the IEEE 118-bus test case with realistic forecast data for the wind farms, and Monte Carlo simulations to evaluate the constraint violations.

1) *Simulation setup*: We use the IEEE 118 bus specifications from [33] with the following modifications: The bus voltage limits are set to 0.94 p.u. and 1.06 p.u. As the upper branch flow limits are specified in MW, the active line flow limit is considered for branch flows. The line flow limits are decreased by 30% and the load is increased by 30% to obtain a more constrained system. Two wind farms with a rated power of 300 MW and 600 MW are placed at buses 5 and 64. Realistic day-ahead wind forecast scenarios from [34] and [35] are used for both wind farms. To create the scenarios, the methodology described in [34] is used. The forecasts are based on wind power measurements in the Western Denmark area from 15 different control zones collected by the Danish transmission system operator Energinet. We select control zone 1 to correspond to the wind farm at bus 5 and zone 7 to the wind

farm at bus 64. We allow a constraint violation of $\epsilon = 5\%$ for all considered approaches. In order to construct the rectangular uncertainty set, the confidence parameter $\beta = 10^{-3}$ is selected. Then, a minimum of 314 scenarios are required according to (45). The forecast is computed as mean value of the scenarios. For the Gaussian uncertainty set, we compute the co-variance matrix based on these scenarios. Fig. 8 shows the forecast data from hour 1 to hour 5 with the upper and lower bounds specified by the maximum and minimum scenario values, respectively. In Fig. 9 the rectangular and Gaussian uncertainty set for hour 4 are shown.

In the following, the parameters for the corrective control policies are specified. The generators at buses $\{12, 26, 54, 61\}$ participate with an equal participation factor of 0.25. Wind farms have a reactive power capability of 0.95 inductive to 0.95 capacitive [27]. The approach using PTDFs assigns a fixed power factor $\cos \phi$ to each wind farm. The affine policy includes a generator voltage and wind farm reactive power corrective control, assigning an updated set-point to generators and wind farms based on the actual realization of the forecast errors. To facilitate comparability, we use the same scenarios for all approaches to compute the respective uncertainty sets. We evaluate the constraint violations using Monte Carlo simulations with 10'000 scenarios and MATPOWER AC power flows. We enable the enforcement of generator reactive power limits in the power flow, i.e. *PV* buses are converted to *PQ* buses once the limits are reached, as otherwise high nonphysical overloading of the limits can occur [36]. Furthermore, we distribute the loss mismatch from the active generator set-points among the generators according to their participation factors and rerun the power flow to mimic the response of automatic generation control.

2) *Numerical Comparison to Alternative Approaches*: In the following, the main modeling assumptions of the respective approaches and the type of chance constraints they include are outlined:

- **Chance-constrained DC-OPF [5] (DC-OPF)**: A robust formulation based on DC-OPF includes chance constraints on active generator power and active branch flow. Interval bounds on the forecast errors are assumed. Hence, we use the scenarios to compute the interval bounds. A power factor of 1 is assumed for the wind farms. Corrective control of active generator set-points is included.
- **Iterative chance constrained AC-OPF [12] (Iterative)**: At each iteration the Jacobian is computed and the uncertainty bounds of the chance constraints are updated until convergence is reached. The forecast errors are assumed to follow a Gaussian distribution. The covariance matrix constructed from the N_s scenarios is used. Chance constraints on active and reactive generator limits, voltage magnitudes and apparent line flows are included in the formulation. A power factor of 1 is assumed for the wind farms, as no reactive power corrective control is included in [12].

These two approaches are compared to the following approaches based on the formulations presented in this work:

TABLE VI
GENERATION COST IN RELATION TO AC-OPF WITHOUT CONSIDERATION
OF UNCERTAINTY – COST OF UNCERTAINTY

Time step (h)	1	2	3	4	5
AP (Rect) (%)	0.774	0.740	0.755	0.921	1.562
PTDF (Rect) (%)	0.785	0.748	0.767	0.931	1.588
DC-OPF [5] (%)	-2.782	-2.826	-2.824	-2.673	-2.165
AP (Gauss) (%)	0.515	0.461	0.467	0.489	0.512
PTDF (Gauss) (%)	0.523	0.468	0.477	0.497	0.520
Iterative [12] (%)	0.519	0.465	0.473	0.494	0.516

- AC-OPF with convex relaxations but without chance-constraints (AC-OPF) [15]
- Chance constrained AC-OPF with convex relaxations, using an affine policy for a Gaussian uncertainty set (AP (Gauss)) including corrective control for wind farms, generator voltages and active power.
- Chance constrained AC-OPF with convex relaxations, using an affine policy for a rectangular uncertainty set (AP (Rect)) including corrective control for wind farms and generator voltages and active power.
- Chance constrained AC-OPF with convex relaxations, using PTDFs (PTDF (Gauss)) for a Gaussian uncertainty set.
- Chance constrained AC-OPF with convex relaxations, using PTDFs (PTDF (Rect)) for a rectangular uncertainty set.

In Table VI the cost of uncertainty for the different approaches and considered time steps are shown. The cost of uncertainty represents the additional cost incurred by considering the stochastic variables, and is defined as the difference between the solution of the chance-constrained and a baseline. In this paper, the AC-OPF with convex relaxations but without considering uncertainty is assumed as the baseline cost. From Table VI, we make the following observations. First, the DC-OPF (with chance-constraints) leads to a cost reduction, as no losses are considered compared to the AC-OPF. Second, the approaches stemming from robust optimization lead to a cost increase of approximately 0.8% for time step 1 compared to an increase of approximately 0.5% for the same time step for the approaches assuming a Gaussian distribution. This shows that the Gaussian uncertainty set is less conservative. For the rectangular uncertainty set, the affine policy reduces the cost compared to the approach using PTDFs. Comparing the approaches for the Gaussian uncertainty set, again the affine policy results to the lowest cost of uncertainty compared to the approach using PTDFs and the iterative chance-constrained AC-OPF. The reason for that is that the affine policy includes corrective control for voltages and both active and reactive power.

In Table VII the violation probability of the chance constraints on active power, voltages, and active branch flows are shown. Monte Carlo simulations using 10'000 scenarios with MATPOWER AC power flows are conducted. A minimum violation limit of 10^{-3} p.u. for active generator limits

TABLE VII
VIOLATION PROBABILITY OF THE CHANCE CONSTRAINTS ON ACTIVE
POWER, VOLTAGES, AND ACTIVE BRANCH FLOW FOR THE FORECAST
DATA. MONTE CARLO SIMULATIONS USING 10'000 SCENARIOS WITH
MATPOWER AC POWER FLOWS ARE CONDUCTED. INSECURE
INSTANCES ARE MARKED IN BOLD.

Time step (h)	1	2	3	4	5
Bus voltage					
AC-OPF (%)	0.0	0.1	0.2	1.0	4.3
DC-OPF [5] (%)	100.0	100.0	100.0	100.0	100.0
PTDF (Rect) (%)	19.5	20.9	14.6	13.0	12.9
AP (Rect) (%)	0.0	0.0	0.0	0.0	0.0
PTDF (Gauss) (%)	20.0	21.2	15.0	13.5	13.0
AP (Gauss) (%)	0.7	1.9	4.3	7.2	7.6
Iterative [12] (%)	0.0	0.0	0.0	0.0	0.0
Active power line limit					
AC-OPF (%)	17.7	18.8	14.9	32.5	46.5
DC-OPF [5] (%)	0.0	0.0	0.0	2.8	0.0
PTDF (Rect) (%)	0.0	0.0	0.0	0.0	0.0
AP (Rect) (%)	0.0	0.0	0.0	0.0	0.0
PTDF (Gauss) (%)	4.6	11.1	13.1	9.3	7.8
AP (Gauss) (%)	4.6	3.7	0.9	2.6	5.8
Iterative [12] (%)	1.6	2.0	3.6	4.2	5.3
Active generator limit					
AC-OPF (%)	46.4	48.8	45.9	45.5	40.9
DC-OPF [5] (%)	34.3	38.6	30.1	14.5	2.0
PTDF (Rect)	0.0	0.0	0.0	0.0	0.0
AP (Rect) (%)	0.0	0.0	0.0	0.0	0.0
PTDF (Gauss) (%)	2.6	3.6	2.8	3.1	5.5
AP (Gauss) (%)	0.0	0.2	0.4	2.3	0.7
Iterative [12] (%)	2.9	4.1	3.0	3.3	5.7

and 0.1% for voltage and line flow limits is considered to exclude numerical errors. In all considered time steps, the AC-OPF without consideration of uncertainty leads to insecure instances and violates constraints on active line and generator limits.

First, investigating the robust approaches using the rectangular uncertainty set the following observations can be made: The robust DC-OPF formulation in [5] leads to insecure instances for all time steps and violates both voltage and generator active power constraints. The approach using PTDFs reduces the voltage violations but does not comply with the 5% confidence interval. The AC-OPF using the affine policy complies with the chance constraints for all time steps while slightly decreasing the generation cost compared to the approach using PTDFs. As the scenario based method is conservative, there are nearly zero violations occurring for the considered 10'000 samples for the approach using the affine policy.

Second, we compare the different approaches which assume a Gaussian distribution of the forecast errors. The affine policy improves upon the approach using PTDFs and results to a

TABLE VIII
COMPARISON OF VIOLATION PROBABILITY OF THE CHANCE
CONSTRAINTS ON ACTIVE POWER, VOLTAGES, AND ACTIVE BRANCH
FLOW FOR AFFINE POLICY AND ITERATIVE CC-AC-OPF WITH 10'000
SAMPLES FROM A GAUSSIAN DISTRIBUTION.

Time step (h)	1	2	3	4	5
Bus voltage					
AP (Gauss) (%)	0.1	0.4	0.5	0.8	0.7
Iterative [12] (%)	0.0	0.0	0.0	0.0	0.0
Active power line limit					
AP (Gauss) (%)	2.2	1.7	2.1	2.1	2.1
Iterative [12] (%)	1.5	1.7	1.7	2.1	2.1
Active generator limit					
AP (Gauss) (%)	2.4	2.7	2.7	2.6	2.5
Iterative [12] (%)	2.7	2.6	2.3	2.4	2.1

secure operation for time steps 1 to 3. For time steps 4 and 5 we observe a slight violation of the active power line and bus voltage limit. This is due to the fact that we do not sample out of a Gaussian distribution but out of a set of realistic forecast scenarios, that apparently are not Gaussian distributed. The iterative approach results to a secure operation for time steps 1 to 4 and slightly violates the active generator and branch flow limit in time step 5.

In order to verify if these violations occur due to the mismatch between actual distribution and the assumed Gaussian we repeat the 10'000 scenario evaluations for both affine policy and the iterative chance-constrained AC OPF from [12]. We sample from the Gaussian distribution assumed for the uncertainty set. The results are shown in Table VIII. For all 5 time steps, both approaches comply with the 5% violation probability. Hence, the occurring violations in Table VII stem from the mismatch between Gaussian distribution and actual probability distribution. As shown in Table VI, the affine policy results in a slightly lower generation cost than the iterative AC OPF, as it includes corrective control policies. This leads us to the following conclusions. First, that if the forecast errors do follow a normal distribution both approaches demonstrate good performance and do not exceed the violation limit. If the data are not normally distributed, as is the case for the results shown in Table VII, none of the two methods can guarantee that the violation probability will be below ϵ . The differences in performance in that case are, as it would be expected, data- and system-specific. However, independent from the fact if the underlying probability distribution is Gaussian or not, one difference that remains is that the approach proposed in this paper is more rigorous, since it provides guarantees regarding the global optimality of the obtained solution and allows to include corrective control policies related to reactive power and voltage.

Table IX lists the penalty weights and obtained near-global optimality guarantees for the five time steps. Note that it is sufficient to define for both uncertainty sets a penalty weight of $\mu = 100$ p.u. to obtain zero relaxation gap, i.e. rank-1 solution

TABLE IX
POWER LOSS PENALTY WEIGHT AND NEAR-GLOBAL OPTIMALITY
GUARANTEES FOR IEEE 118 BUS TEST CASE

	Penalty weight μ (p.u.)	Near-global optimality guarantee δ_{opt} (%)
AP (Rect)	100	≥ 99.99
AP (Gauss)	100	≥ 99.99

TABLE X
SOLVING TIME FOR IEEE 118 BUS TEST CASE

AP (Rect)	AP (Gauss)	PTDF (Rect)
30 sec	10 min	15 sec
PTDF (Gauss)	DC-OPF [5]	Iterative [12]
15 sec	≤ 1 sec	4 sec

matrices and a near-global optimality guarantee of larger than 99.99%, i.e. the maximum deviation from the global optimum is smaller than 0.01% of the objective value.

Table X lists the computational time of the different approaches. The optimization problems are solved on a desktop computer with an Intel Xeon CPU E5-1650 v3 @ 3.5 GHz and 32 GB RAM. For all optimization problems except the iterative approach, MOSEK V8 [31] is used. The iterative approach utilizes the MATPOWER AC-OPF. The DC-OPF formulation is the fastest, as the optimization problem is a linear program. The computational time increases with increasing constraint complexity. The SOC constraints in the formulation for the Gaussian uncertainty set are computationally the most challenging. We observe that the iterative approach, despite the need for computing a number of iterations, converges faster than all approaches that utilize convex relaxations and an SDP solver. Current trends expect the need of more rigorous optimal power flow approaches in the future, that e.g. can guarantee a global minimum. In that case the need for further research to improve both the optimization solvers and the convex formulations of the AC-OPF problem is apparent.

VI. DISCUSSION AND OUTLOOK

a) *Computation speed:* As shown in Table X and discussed in the previous section, the computation speed of the SDP approaches might present some challenges for certain systems or certain formulations. SDP solvers are still under continuous development and they are expected to reach the maturity of the linear programming solvers in the following several years. Given that current trends lead us to more rigorous approaches for optimization in power systems, and the continuous development of better solvers, we expect that potential computational bottlenecks will be substantially reduced in the near future. At the same time, appropriate problem formulations are necessary in order to boost computational speed and improve scalability. Possible directions to increase the computational speed of the proposed approaches are decomposition techniques and distributed optimization. The chordal decomposition technique, outlined in [23], [37], can be

applied to W_0 and B_i matrices to decrease the computational burden of the semidefinite constraints (18). A different method is the alternating direction method of multipliers (ADMM) for sparse semidefinite problems, which allows to parallelize the optimization and utilize a high performance computer [38]. We intend to investigate these techniques for our proposed approaches in future work.

b) Gaussian distribution: Over the last years, there have been discussions in the power systems community if the forecast errors can be accurately represented by Gaussian probability distributions. As shown in this paper, and specifically in Table VII, we observed that all approaches that assumed a Gaussian probability distribution for the forecast error, during 1 or 2 instances resulted in violations that exceeded the 5% constraint violation limit. On the contrary, the piecewise affine policy with the rectangular uncertainty set never exceeded the constraint violation limit. Although we also believe that Gaussian distributions might not always be the most appropriate distribution to model forecast errors, they still exhibit certain benefits. Assuming a Gaussian distribution can be very convenient when there is insufficient amount of data at hand, as it can provide a good first approximation of the power system operation under uncertainty. At the same time, through the covariance matrix, with Gaussian distribution we can capture geographical correlations between wind farms, solar PV plants, or other types of uncertainty. Given also that, as proposed in this paper, there is an analytical reformulation of the Gaussian chance constraints for the OPF problem, it can be a helpful tool for the community.

c) Relaxation gap: A very active research topic currently is the identification of the conditions under which we can obtain a zero relaxation gap for the SDP reformulation of the OPF problem. There is extensive literature demonstrating how the SDP reformulation succeeds, while there are also research papers showing the limitations of this approach. In our approach, we had to introduce a power loss penalty factor to obtain a tight relaxation for the original non-linear OPF problem. As shown in Fig. 5 and in Fig. 6, for a certain (large) range of values for the penalty factor, we could always obtain a zero relaxation gap. In our future work, we intend to further investigate the properties of this penalty factor and the conditions under which we can always obtain a zero relaxation gap. For example, had we assumed a renewable curtailment cost, this (in the extreme case) could introduce negative linear costs, which may or may not result in a tight relaxation.

d) Security-constrained OPF: The convex chance-constrained AC-OPF formulation, as proposed in this paper, is only one of the components – although possibly one of the most fundamental ones – required for power system operation. According to current practice, system operators are expected to operate the system in an N-1 secure state, and for that a Security-Constrained OPF is necessary. As it might become apparent, the formulation proposed in this paper can become a central component for that tool.

In general, there are two main approaches to include security constraints in OPF. The first is the iterative approach. The operator defines a set of critical contingencies, that ensure that the system is N-1 secure against them. First, the OPF is solved

without security constraints. Subsequently, for the determined optimal operating point, the operator runs an AC power flow for each critical contingency and checks if any limits are violated. If not, then the algorithm stops and the determined optimal set-point corresponds also to the N-1 secure dispatch. If there are limits that are violated, then these are added as constraints to original OPF problem, and we resolve the OPF. We iterate until we determine an operating point that does not violate any limits for any critical contingency.

An alternative approach is to include all relevant security constraints directly in the OPF formulation. In that case, we have to append the set of our optimization variables with additional variables that correspond to the contingency cases. This becomes computationally more expensive. The security constraints can be included in the proposed formulation by defining a matrix $W^s(\zeta)$ for each outage s of a generation unit, transmission line or wind farm.

In an N-1 context, uncertainty can be treated exactly as described for the N-0 case in this paper. With the difference, of course, of either tightening each constraint iteratively, or expanding the optimization problem with additional optimization variables and constraints. Although still a convex problem, for large systems such a problem can become very computationally expensive and possibly intractable. Improving the scalability and tractability of SDP approaches is still an active research topic, as we discussed at the beginning of this Section. In future work, we plan to address topics related to convex relaxations for the Security-Constrained OPF under uncertainty.

VII. CONCLUSIONS

In this work, a convex formulation for a chance-constrained AC-OPF is presented which is able to provide near-global optimality guarantees. The OPF formulation considers chance constraints for all relevant state variables, and has an explicit representation of corrective control policies. Two tractable formulations are proposed: First, a scenario-based method is applied in combination with robust optimization. Second, assuming a Gaussian distribution of forecast errors, we provide an analytical reformulation of the chance constraints. Detailed case studies on the IEEE 9, 24 and 118-bus test systems are presented. For the 118-bus case, we used realistic forecast data and Monte Carlo simulations to evaluate constraint violations. Compared to a chance-constrained DC-OPF formulation, we find that the formulations proposed in this paper are more accurate and significantly decrease constraint violations. Compared with iterative non-convex AC-OPF formulations, because our approach enables corrective control actions, we find that it results to lower generation costs, while both our piece-wise affine control policy and the iterative AC-OPF do not exceed the constraint violation limit for the Gaussian uncertainty set. Most importantly, with our proposed approach, we obtain tight near-global optimality guarantees which ensure that the distance to the global optimum is smaller than 0.01% of the objective value. Further work will focus on (i) N-1 security (ii) chordal decomposition techniques and (iii) integration of controllability of HVDC.

ACKNOWLEDGMENT

The authors would like to thank Pierre Pinson for sharing the forecast data, Line Roald for providing an updated version of the code from [12], and Martin S. Andersen and Daniel K. Molzahn for fruitful discussions.

REFERENCES

- [1] A. Nemirovski and A. Shapiro, "Convex approximations of chance constrained programs," *SIAM Journal on Optimization*, vol. 17, no. 4, pp. 969–996, 2006.
- [2] D. Bienstock, M. Chertkov, and S. Harnett, "Chance-constrained optimal power flow: Risk-aware network control under uncertainty," *SIAM Review*, vol. 56, no. 3, pp. 461–495, 2014.
- [3] L. Roald, F. Oldewurtel, T. Krause, and G. Andersson, "Analytical reformulation of security constrained optimal power flow with probabilistic constraints," in *IEEE PowerTech*, Grenoble, France, 2012.
- [4] M. Lubin, Y. Dvorkin, and S. Backhaus, "A robust approach to chance constrained optimal power flow with renewable generation," *IEEE Transactions on Power Systems*, vol. 31, no. 5, pp. 3840 – 3849, 2016.
- [5] R. A. Jabr, S. Karaki, and J. A. Korbane, "Robust multi-period OPF with storage and renewables," *IEEE Transactions on Power Systems*, vol. 30, no. 5, pp. 2790–2799, 2015.
- [6] L. Roald, S. Misra, T. Krause, and G. Andersson, "Corrective control to handle forecast uncertainty: A chance constrained optimal power flow," *IEEE Transactions on Power Systems*, vol. 32, no. 2, pp. 1626–1637, 2017.
- [7] S. S. Guggilam, E. Dall'Anese, Y. C. Chen, S. V. Dhople, and G. B. Giannakis, "Scalable optimization methods for distribution networks with high PV integration," *IEEE Transactions on Smart Grid*, vol. 7, no. 4, pp. 2061 – 2070, 2016.
- [8] K. Baker, E. Dall'Anese, and T. Summers, "Distribution-agnostic stochastic optimal power flow for distribution grids," in *North American Power Symposium (NAPS)*, Denver, US, 2016.
- [9] T. Summers, J. Warrington, M. Morari, and J. Lygeros, "Stochastic optimal power flow based on convex approximations of chance constraints," in *2014 Power Systems Computation Conference*, Aug 2014, pp. 1–7.
- [10] E. D. Anese, K. Baker, and T. Summers, "Chance-constrained AC optimal power flow for distribution systems with renewables," *IEEE Transactions on Power Systems*, vol. PP, no. 99, pp. 1–1, 2017.
- [11] H. Zhang and P. Li, "Chance constrained programming for optimal power flow under uncertainty," *IEEE Transactions on Power Systems*, vol. 26, no. 4, pp. 2417–2424, 2011.
- [12] J. Schmidli, L. Roald, S. Chatzivasileiadis, and G. Andersson, "Stochastic AC optimal power flow with approximate chance-constraints," in *IEEE Power and Energy Society General Meeting*, Boston, US, 2016.
- [13] K. Dvijotham and D. K. Molzahn, "Error bounds on the DC power flow approximation: A convex relaxation approach," in *2016 IEEE 55th Conference on Decision and Control (CDC)*, Dec 2016, pp. 2411–2418.
- [14] S. V. Dhople, S. S. Guggilam, and Y. C. Chen, "Linear approximations to AC power flow in rectangular coordinates," in *2015 53rd Annual Allerton Conference on Communication, Control, and Computing (Allerton)*, Sept 2015, pp. 211–217.
- [15] J. Lavaei and S. H. Low, "Zero duality gap in optimal power flow problem," *IEEE Transactions on Power Systems*, vol. 27, no. 1, pp. 92–107, 2012.
- [16] R. A. Jabr, "A conic quadratic format for the load flow equations of meshed networks," *IEEE Transactions on Power Systems*, vol. 22, no. 4, pp. 2285–2286, 2007.
- [17] X. Bai, H. Wei, K. Fujisawa, and Y. Wang, "Semidefinite programming for optimal power flow problems," *International Journal of Electrical Power & Energy Systems*, vol. 30, no. 6, pp. 383–392, 2008.
- [18] B. C. Lesieutre, D. K. Molzahn, A. R. Borden, and C. L. DeMarco, "Examining the limits of the application of semidefinite programming to power flow problems," in *2011 49th Annual Allerton Conference on Communication, Control, and Computing (Allerton)*, Sept 2011, pp. 1492–1499.
- [19] R. Madani, S. Sojoudi, and J. Lavaei, "Convex relaxation for optimal power flow problem: Mesh networks," *IEEE Transactions on Power Systems*, vol. 30, no. 1, pp. 199–211, 2015.
- [20] M. B. Cane, R. P. O'Neill, and A. Castillo, "History of optimal power flow and formulations," Federal Energy Regulatory Commission, 2012.
- [21] M. Vrakopoulou, M. Katsampani, K. Margellos, J. Lygeros, and G. Andersson, "Probabilistic security-constrained AC optimal power flow," in *IEEE PowerTech*, Grenoble, France, 2012.
- [22] K. Margellos, P. Goulart, and J. Lygeros, "On the road between robust optimization and the scenario approach for chance constrained optimization problems," *IEEE Transactions on Automatic Control*, vol. 59, no. 8, pp. 2258–2263, 2014.
- [23] D. K. Molzahn, J. T. Holzer, B. C. Lesieutre, and C. L. DeMarco, "Implementation of a large-scale optimal power flow solver based on semidefinite programming," *IEEE Transactions on Power Systems*, vol. 28, no. 4, pp. 3987–3998, 2013.
- [24] A. Ben-Tal and A. Nemirovski, "Selected topics in robust convex optimization," *Mathematical Programming*, vol. 112, no. 1, pp. 125–158, 2008.
- [25] Ibraheem, P. Kumar, and D. P. Kothari, "Recent philosophies of automatic generation control strategies in power systems," *IEEE Transactions on Power Systems*, vol. 20, no. 1, pp. 346–357, 2005.
- [26] H. Vu, P. Pruvot, C. Launay, and Y. Harmand, "An improved voltage control on large-scale power system," *IEEE transactions on power systems*, vol. 11, no. 3, pp. 1295–1303, 1996.
- [27] M. Tsili and S. Papathanassiou, "A review of grid code technical requirements for wind farms," *IET Renewable Power Generation*, vol. 3, no. 3, pp. 308–332, 2009.
- [28] A. Nemirovski, "On safe tractable approximations of chance constraints," *European Journal of Operational Research*, vol. 219, no. 3, pp. 707–718, 2012.
- [29] S. Chatzivasileiadis, T. Krause, and G. Andersson, "Flexible AC transmission systems (FACTS) and power system security - A valuation framework," in *IEEE Power and Energy Society General Meeting*, Detroit Michigan, US, 2011.
- [30] M. Lubin and I. Dunning, "Computing in operations research using Julia," *INFORMS Journal on Computing*, vol. 27, no. 2, pp. 238–248, 2015.
- [31] MOSEK ApS, *MOSEK 8.0.0.37*, 2016.
- [32] R. D. Zimmerman, C. E. Murillo-Sánchez, and R. J. Thomas, "MATPOWER: Steady-state operations, planning, and analysis tools for power systems research and education," *IEEE Transactions on Power Systems*, vol. 26, no. 1, pp. 12–19, 2011.
- [33] "IEEE 118-bus, 54-unit, 24-hour system,," Electrical and Computer Engineering Department, Illinois Institute of Technology, Tech. Rep. [Online]. Available: http://motor.ece.iit.edu/data/JEAS_IEEE118.doc
- [34] P. Pinson, "Wind energy: Forecasting challenges for its operational management," *Statistical Science*, pp. 564–585, 2013.
- [35] W. A. Bukhsh, C. Zhang, and P. Pinson, "An integrated multiperiod OPF model with demand response and renewable generation uncertainty," *IEEE Transactions on Smart Grid*, vol. 7, no. 3, pp. 1495–1503, May 2016.
- [36] A. E. Efthymiadis and Y. H. Guo, "Generator reactive power limits and voltage stability," in *Fourth International Conference on Power System Control and Management (Conf. Publ. No. 421)*, 1996, pp. 196–199.
- [37] L. Vandenberghe and M. S. Andersen, "Chordal graphs and semidefinite optimization," *Foundations and Trends® in Optimization*, vol. 1, no. 4, pp. 241–433, 2015.
- [38] R. Madani, A. Kalbat, and J. Lavaei, "ADMM for sparse semidefinite programming with applications to optimal power flow problem," in *2015 54th IEEE Conference on Decision and Control (CDC)*, Dec 2015, pp. 5932–5939.